The R Stars: Carbon Stars of a Different Kind

Robert D. McClure
Dominion Astrophysical Observatory, Herzberg Institute of Astrophysics,
National Research Council, Canada, 5071 W. Saanich Road, Victoria, BC, V0S 1N0
Electronic mail: mcclure@dao.nrc.ca

ABSTRACT

After ∼16 years of radial-velocity observations of a sample of 22 R-type carbon stars, no evidence for binary motion has been detected in any of them. This is surprising considering that approximately 20% of normal late-type giants are spectroscopic binaries, and the fraction is close to 100% in barium, CH, and subgiant/dwarf CH and barium stars. It is suggested, therefore, that a process that has caused the mixing of carbon to the surface of these stars cannot act in a wide binary system. Possibly, the R stars were once all binaries, but with separations that would not allow them to evolve completely up the giant and asymptotic giant branchs without coalescing. This coalescence may be the agent which causes carbon produced in the helium-core flash to be mixed outwards to a region where convection zones can bring it to the surface of the star.

1. Introduction

The Henry Draper classification divided carbon stars into two groups N and R on the basis of their spectral features. The N stars exhibit very strong depression of light in the violet part of the spectrum. They are the classical carbon stars that are most easily detected in infrared surveys and used as tracers of an intermediate age population in extragalactic objects. The R stars, on the other hand, have warmer temperatures, and blue/violet light is accessible to observation, and atmospheric analysis.

The most extensive analysis of the R stars has been done by Dominy (1984), who found that in the warm R0−R4 stars, C is overabundant on average by approximately 0.7 dex relative to the sun and to normal G and K giants. On the other hand he found that the O abundance is normally near solar, and the N abundance just slightly enhanced. At CNO cycle equilibrium both C and O are depleted substantially. The lack of oxygen and carbon depletion, therefore, led Dominiy to the conclusion that the CNO cycle operating near equilibrium is not responsible for the fact that C/O $>$ 1 in these stars. The excess carbon has to come from some other process.

Dominy also found that the s process element abundances are nearly solar, similar to results of Gordon (1968), and Green et al. (1973). This is in sharp contrast with most other carbon and carbon-related stars (see reviews by McClure 1984a, 1985). The N, S, barium, CH, sgCH, and dwarf carbon stars all have significantly enhanced abundances of the s process elements relative to iron (e.g., Lambert 1985; Green and Margon 1994). The N stars and many of the S stars are assumed to have undergone helium-shell flashing on the asymptotic giant branch (AGB), and the third dredge-up phase has brought carbon and s process elements to the surface (e.g., see Iben and Renzini 1983).

Like many of the barium, CH, sgCH and dwarf carbon stars, the warmer R stars are too faint to be on the AGB. Scalo (1976) has reviewed the status of various carbon-related stars in the Hertzsprung-Russell diagram, and has pointed out that the R0−R4 stars lie in a similar temperature/luminosity domain as the

barium stars. They are well below the lower luminosity boundary of the onset of helium shell flashing. The lack of s process enhancement, and low luminosity led Dominy (1984) to conclude that the R stars probably received their enhanced carbon from the helium-core flash at the tip of the first ascent giant branch. This still remains the most viable hypothesis, although it is not known how the core-flash contaminants have been mixed to the surface of the star.

2. Rationale for Radial Velocity Surveys of Carbon-Related Stars

In the late 1970's, it had become apparent that the classical carbon stars could be explained by helium-shell flashing on the AGB, whereas many of the other stars with enhanced carbon could not, because they were too faint for AGB evolution. McClure (1979), suggested the possibility that the CH stars were binaries, because in globular clusters they tended to be found only in ones of very low central concentration where binaries may not be disrupted as easily. A velocity survey of the barium stars quickly led to the conclusion that all barium stars are binaries (McClure, Fletcher and Nemec 1980), and later surveys showed that CH stars as well as barium stars are all binaries (McClure 1983, 1984b), presumably having undergone mass-transfer episodes. These results were confirmed by observations of Jorissen and Mayor (1988), who also showed that a large fraction of S stars are binaries. The latter stars are found to belong to two groups (e.g. Brown et. al. 1990 and references therein). Those that exhibit the radioactive s process element Tc are single AGB stars undergoing helium-shell flashing that is slowly raising the C/O ratio to greater than unity. Those that do not exhibit Tc are found to be all binaries that have received material contaminated with C and s process elements from a companion that had undergone helium-shell flashing on the AGB. Thus a binary mass-transfer hypothesis has explained most of the carbon-related objects that are either too faint to be on the AGB, or that do not exhibit radioactive Tc, which has a half life that is a good fraction of a star's lifetime on the AGB. The peculiar abundances in these stars all originated from the AGB.

The warmer R stars suffer the same problem in our understanding that we had in the late 1970's for the barium and CH stars. They are too faint to be AGB stars. Therefore, when it was found that barium stars were likely all binaries, a survey was begun of radial velocities of the R stars also. Note, however, that at that time the s process abundance of the R stars was unclear. Therefore, it was considered quite possible that the R stars would fit into the same AGB − carbon star connection as the barium and CH stars.

3. The Stellar Sample, and Radial Velocity Observations

A sample of 38 R stars (based on their HD classes) was picked, mostly from the compilation by Yamashita (1972), who examined spectra of a large number of carbon stars, and identified strengths of various bands and lines for each star. Among the R stars, the warmer R0−R4 stars are the most similar to normal giants, and less likely to exhibit velocity "jitter" characteristic of more luminous giants which have more extended and less stable atmospheres. Mostly R0−R4 stars were included in the sample, therefore, but a few R5-R9 stars were also observed. The problems of sorting out other types that may contaminate the sample (in particular the CH stars) will be discussed below.

The observations were performed using the radial-velocity spectrometer on the 1.2-m telescope of the Dominion Astrophysical Observatory in Victoria (see Fletcher et al. 1982; McClure et al. 1985 for descriptions of the instrument). Although this instrument is capable of a precision of about $\pm$ 0.3 km s^{-1}, because of the faintness of the R stars and the limited time spent per observation, the final errors were

larger than this. From repeated observations, the standard deviation of a single observation was found to be on the average ± 0.62 km s^{-1}. The radial-velocity values and Julian dates (-2400000^d) for all observations in the sample are listed in Table 1.

It is very difficult to pick a pure sample of a particular type of carbon star because they are defined by spectral characteristics which may be difficult to detect at low dispersion, and these characteristics sometime overlap between different stellar-population types. The approach taken here was to select a fairly large sample of stars that had been classified as type R, and worry later about sorting out misclassified objects, when better data and classifications became available. Unfortunately, as a result of this, some non-R stars have been included in my previous preliminary estimates of binary frequency (e.g., McClure 1989). The final adopted classifications for stars in the sample are listed in Table 2.

3.1. The N stars and R5-R9 stars:

With the most recent classifications, especially those of Keenan (1993) and Barnbaum et al. (1996), there are four stars in the sample that should be rejected because they are N stars. The velocities for these four stars are shown at the top of Figure 1. The scatter in velocities for each of them is significantly greater than the precision of the spectrometer, and greater than the scatter for the true R stars in the sample. The average of the standard deviations of the individual observations is $\pm$ 1.62 km s^{-1}. However, there is no evidence for long-term binary motion, the scatter being just a "jitter" which is typical for high luminosity stars with extended atmospheres (e.g., Pryor et al. 1988).

Eight stars in the sample are classified as R5-R9, and the velocity data for these are shown in the middle part of Figure 1. These stars again are well up on the giant branch, and they exhibit a similar velocity jitter. The average of the standard deviations for the individual observations in this case is $\pm$ 1.60 km s^{-1}. Again, there is no convincing evidence for binary motion. The star with the largest deviations, HD 59643, is the coolest star in the sample, with a classification of R9.

3.2. The CH Stars

The problem of distinguishing between CH stars and R stars is a very difficult one, especially if the spectra are at rather low resolution as is the case for many of these stars. It is very important that this be done, however, because the CH stars have been shown to be binaries (McClure 1984b), and since we are trying to determine the binary frequency for the R stars here, we do not want CH binaries contaminating the sample. The CH stars were mostly classified as R stars before they were recognized as a separate class by Keenan (1942). The main distinguishing spectral features are very strong CH bands, enhanced lines of s process elements and weaker Fe group elements as well as various strengths of C_2 bands. Many R stars also have quite strong CH, however (see Yamashita 1972, Figure 10e), and at low dispersion where the strengths of narrow lines are difficult to estimate, a CH star may look very similar to an R star. The CH stars are mostly high-velocity-halo objects, whereas the R stars belong to the low-velocity-old-disk population (McLeod 1947). Therefore, any high-velocity object can normally be assumed to be a CH star. There are, however, a few low velocity CH stars, which Yamashita (1975a) has identified spectroscopically, and referred to as "CH-like" stars. Their spectra appear to be identical to the CH stars. If stars of this type are misclassified as R stars, they will contaminate the sample, and may affect the estimation of binary frequency.

One star, HD 16115, which has been classified by Yamashita (1975a), and by Keenan (1993) as a CH-like star, has been kept in the R star list on the basis of its s process and Fe abundance. Although CH bands are strong, Dominy (1984) finds a nearly normal abundance at high dispersion for both the s process elements and Fe in this star, and this is one of the main distinguishing features between a CH and an R classification.

Four other stars, whose velocities are exhibited at the bottom of Figure 1, have been classified as CH or CH-like. HD 85066 remained with an R3 classification in the compilation by Yamashita (1972), although it exhibits his strongest CH index value. Hartwick and Cowley (1985), on the other hand, have classified it more recently at higher resolution as a CH star. This star is a definite binary with a period of 2902 days. The other three stars have been classified as CH-like by Yamashita (1975a). BD +2°3336 is a definite binary with a period of 446 days. BD +29°95 exhibits erratic velocity behavior, although it cannot be due to long term binary motion. Perhaps there has been a difficulty with identification on some nights at the telescope, but because it is not an R star, it is not important for the present subject. One other CH-like star HD 197604 shows no evidence for binary motion. If one neglects BD +29°95, two out of three CH-like stars are binaries, which is not inconsistent with the high binary frequency of their high-velocity counterparts.

Orbital elements are listed in Table 3 for the two CH stars that are definite binaries. The velocities as a function of phase, resulting from the orbital solutions are plotted in Figure 2.

3.3. The R0−R4 Stars

The velocities for the remaining 22 R0−R4 stars are shown in Figure 3. The range of dates in the plots is from mid-1979 to mid-1996.

4. The Binary Frequency of the R Stars

One would be hard pressed to see any evidence for binary motion from these R0−R4 star data. This is surprising considering that the binary frequency for normal G-K giants appears to be of the order of 20%.

Gunn and Griffin (1979) comment that in their velocity observations of field giants, about 30% of stars are variable with amplitudes of a few km s^{-1} over times scales of a few years. Mermilliod and Mayor (1992) have carried out the most extensive systematic velocity program for binary detection among late-type giants, having surveyed numerous stars in 177 open clusters. They find 187 binaries among 905 giants, or a frequency of ∼21%. Monitoring of a small random sample of 39 K giants by the present author, the same sample as discussed in Harris and McClure (1983) supplemented by more recent observations, shows six binaries, or a frequency of 15%.

Comparing zero binaries among 22 R stars, with this large combined sample of normal giant stars, one can carry out a χ^2 test of homogeneity in a 2×2 contingency table (Johnson and Bhattacharyya 1985). This gives a χ^2 of 5.621, indicting that the possibility that the R stars have a normal binary frequency can be rejected at the 98% confidence level! If one were to retain R5 stars in the sample, this would provide five more non-binaries, since even with the small velocity jitter in these, long term velocity variation can be ruled out. They just add to the significance of this result.

5. The R Stars as Coalesced Binaries?

It appears very likely that some process that produces carbon in the atmospheres of R stars cannot operate in a binary system, or alternatively, causes any original binary companion to disappear. The first possibility seems remote. It is difficult to think of such a process that will operate in single stars but not in wide binary systems. Likely, given the luminosities of the warmer R stars, the process in question is one that mixes helium-core-flash material to the surface of the star. Possibly the R stars were all binaries at one time, and the process in question caused the disappearance of their companions. The most likely event would be the coalescence of a binary system that had a separation of components that was too small for evolution up the giant and asymptotic branches to proceed normally. Coalescence perhaps causes mixing in the vicinity of the core during or after the helium-core flash.

Smith and Demarque (1980) discuss the effects of mixing at the core flash in the context of trying to explain the existence of the sgCH stars. They showed that the star becomes fainter than the normal horizontal branch as hydrogen is mixed into the core. During the second ascent up the giant branch, convection zones might then reach down to bring the carbon produced in the flash up to the surface. They concluded that the sgCH stars were too faint to be explained in this manner. However, the R stars are significantly brighter than this, and Smith and Demarque's analysis could very well apply to them, with coalescence of a companion being the process that causes the mixing. If the R stars are produced in this way, one would expect no subgiant or dwarf R stars, and this does appear to be the case. The subgiant and dwarf carbon-related stars that have been analyzed all have enhanced s process elements (Green and Margon 1994; Bond, private communication), unlike the R stars.

One might expect, given the present hypothesis, that the resulting star should be rotating. Angular momentum would be gained by the stellar atmosphere from the orbital energy of the companion spiraling in to the center of the R star. For this reason, observations were made in July 1996 to measure the width of spectral lines in several R stars, and in normal K giants for comparison. Cross-correlation line profiles of these stars were observed with the same radial-velocity spectrometer which was used for the radial-velocity measurements, but care was taken to obtain a complete profile including continuum on each side of the line. Figure 4 shows this comparison for two R stars (dots) relative to two K giants (solid curves). There is no evidence for rotational broadening of the R star profiles, so that this must be taken into account in any binary evolution explanation. Angular momentum gained by a model stellar atmosphere must be dissipated or transferred inwards for this hypothesis to remain viable.

I wish to thank Doug Bond, Murray Fletcher, Les Saddlemyer, and Frank Younger for help over the years in operation of the telescope and radial-velocity spectrometer. I thank Jim Hesser, Chad Hogan, Les Saddlemyer, and Andy Woodsworth for contributing observations to this project over the years. I also thank Chris Tout for very useful discussions.

REFERENCES

Barnbaum, C., Stone, R. P. S., and Keenan, P. C. 1996, preprint

Brown, J. A., Smith, V. V., Lambert, D. L., Dutchover, E. Jr., Hinkle, K. H., and Johnson, H. R. 1990, AJ, 99, 1930

Dominy, J. F. 1984, ApJS, 55, 27

Fletcher, J. M., Harris, H. C., McClure, R. D., and Scarfe, C. D. 1982, PASP, 94, 1017

Green, P. T., and Margon, B. 1994, ApJ, 423, 723

Green, T. F., Perry, J., Snow, T. P. and Wallerstein, G. 1973, A&A, 22, 293

Gordon, C. P. 1968, ApJ, 153, 915

Gunn, J. E., and Griffin, R. F. 1979, AJ, 84, 752

Harris, H. C., and McClure, R. D. 1983, ApJ, 265, L77

Hartwick, F. D. A., and Cowley, A. P. 1985, AJ, 90, 2244

Iben, Jr., and Renzini, A. 1983, ARA&A, 21, 271

Johnson, R. A., and Bhattacharyya, G. K. 1985, in Statistics, Principles and Methods (New York: Wiley), p. 519

Jorissen, A., and Mayor, M. 1988, A&A, 198, 187

Keenan, P. C. 1942, ApJ, 96, 101

Keenan, P. C. 1993, PASP, 105, 905

Lambert, D. L. 1985, in Cool Stars with Excesses of Heavy Elements, eds. M. Jaschek and P. C. Keenan (Dordrecht: Reidel), p. 191

McClure, R. D. 1979, Mem. Soc. Astr. Italiano, 50, 15.

McClure, R. D. 1983, ApJ, 268, 264

McClure, R. D. 1984a, PASP, 96, 117

McClure, R. D. 1984b, ApJ, 280, L31

McClure, R. D. 1985, JRASC, 79, 277

McClure, R. D. 1989, in Evolution of Peculiar Red Giant Stars, eds. H. R. Johnson and B. Zuckerman (Cambridge: Cambridge Univ. Press), p. 196

McClure, R. D., Fletcher, J. M., and Nemec, J. M. 1980, ApJ, 238, L35

McClure, R. D., Fletcher, J. M., Grundmann, W. A., and Richardson, H. E. 1985, in Stellar Radial Velocities, IAU Colloq. 88, eds. A. D. G. Philip, and D. W. Lathem (Schenectady: L. Davis Press), p. 49

McLeod, N. W. 1947, ApJ, 105, 390

Mermilliod, J.-C., and Mayor, M. 1992, in Binaries as Tracers of Star Formation, eds A. Duquennoy, and M. Mayor (Cambridge: Cambridge Univ. Press), p. 183

Pryor, C., Lathem, D. W., and Hazen, M. L. 1988, AJ, 96, 123

Sanford, R. F. 1944, ApJ, 99, 145

Scalo, J. M. 1976, ApJ, 206,474

Shane, C. D. 1928, Lick Obs. Bull., 13, 123

Smith, J. A., and Demarque, P. 1980, A&A, 92, 163

Stephenson, C. B. 1973, Pub. Warner and Swasey Obs., 1, No. 4

Vandervort, G. L. 1958, AJ, 63, 477

Yamashita, Y. 1972, Ann. Tokyo Astr. Obs., 13, 169

Yamashita, Y. 1975a, PASJ, 27, 327

Yamashita, Y. 1975b, Ann. Tokyo Astr. Obs., 15, 47

Table 1. Radial Velocity Data

JD −2400000	RV km s^{-1}	JD −2400000	RV km s^{-1}	JD −2400000	RV km s^{-1}	JD −2400000	RV km s^{-1}	JD −2400000	RV km s^{-1}
HD 1994		**HD 16115**		**BD+23 601**		**HD 57884**		**HD 63353**	
44876.832	−47.68	49241.027	15.50	46714.855	−11.43	45384.773	51.18	45367.895	16.87
44935.809	−45.81	49262.000	15.26	47031.934	−12.26	45410.754	51.63	45384.797	18.53
44967.824	−46.64	49695.727	15.94	47086.910	−11.67	45613.023	51.12	45410.777	20.94
45207.941	−43.94	50142.664	15.85	47196.730	−11.10	45669.953	50.58	45452.758	16.55
45384.668	−46.07			47789.930	−11.49	45712.805	49.08	45668.062	20.20
45583.988	−46.28	**HD 19557**		47872.855	−11.10	46467.781	49.56	47086.953	20.87
45597.906	−45.51	44184.957	−8.03	48950.984	−11.65	46715.023	50.40	47260.777	18.87
45669.734	−44.44	44198.855	−10.10	49695.844	−11.27	47872.965	50.47	47873.000	18.66
45989.758	−43.33	44331.742	−10.91	50129.742	−11.43	50126.816	50.38	50123.879	20.73
46341.773	−46.44	44493.855	−13.31			50127.816	48.31	50128.809	21.24
46657.977	−46.43	44606.969	−12.90	**HD 34467**		50142.754	49.06		
46990.934	−44.79	44876.930	−10.96	45384.754	16.59			**HD 76846**	
47086.832	−45.89	44935.863	−10.83	45410.770	17.75	**HD 58337**		44304.820	25.60
47141.754	−45.86	45051.711	−11.07	45598.020	17.51	45367.879	−1.97	44331.797	25.13
47763.949	−43.28	45207.992	−8.64	45669.984	19.33	45384.812	−1.42	44607.910	24.89
47872.797	−45.83	45283.961	−9.99	45712.836	15.67	45410.805	−1.32	44668.859	24.58
48467.934	−46.38	45384.730	−9.94	46467.758	16.48	45613.000	−1.76	44683.855	25.06
49261.859	−46.02	45410.719	−10.56	46714.887	17.11	45670.055	−2.05	44712.723	25.01
49647.754	−46.19	45597.965	−9.78	47086.918	17.92	45712.863	−0.53	45053.848	24.88
49695.688	−45.01	45669.961	−11.40	48950.977	18.00	46497.812	−0.45	45284.012	24.80
50129.625	−47.30	45989.828	−9.83	49270.055	17.13	46715.043	−1.96	45367.898	24.82
		46341.816	−9.48			47260.719	−1.49	45410.852	25.04
BD+29 95		46714.836	−10.72	**HD 37212**		47873.012	−1.18	45668.070	24.59
45597.934	17.83	47005.953	−10.70	45598.031	33.19	50123.766	−1.57	45712.898	24.61
45669.746	5.98	47086.895	−11.46	45669.945	33.20	50142.789	−0.80	45852.727	25.17
47086.844	17.40	47196.703	−10.89	45712.824	31.13			46110.906	24.76
47763.988	18.32	47214.715	−12.22	46467.805	32.22	**HD 58364**		46937.758	23.52
47872.785	18.68	47789.941	−9.41	46715.008	28.42	45367.871	−8.85	47086.961	24.25
49240.840	−12.20	47872.812	−9.91	47087.043	34.39	45384.820	−7.82	47260.789	24.97
49261.914	17.85	49262.023	−9.97	47872.891	28.03	45410.809	−7.03	47873.051	24.23
49647.785	23.18	49695.762	−12.94			45613.008	−9.13	48951.039	24.36
49695.707	23.05	50129.688	−6.86	**BD+33 1194**		45670.062	−7.27	50128.820	24.71
				45598.027	−57.77	45712.867	−8.36		
BD+21 64		**HD 19881**		45669.996	−57.59	46497.812	−8.10	**HD 77234**	
44876.840	13.94	45384.742	10.49	45712.852	−57.21	46715.047	−8.79	44304.852	4.70
44935.777	14.01	45410.734	12.37	46467.773	−56.56	47086.938	−10.19	44331.805	4.53
45207.945	9.66	45597.973	11.19	46714.949	−57.93	47260.723	−7.85	44382.770	5.45
45384.688	12.29	45669.969	11.64	47031.969	−58.40	47873.023	−8.22	44607.926	6.13
45597.945	12.46	45989.840	13.10	47086.922	−57.86	50123.785	−9.52	44668.910	7.40
45669.762	12.29	46467.695	11.71	47872.949	−57.85	50142.805	−9.49	44683.871	5.07
45989.820	11.71	46714.848	12.77	48950.969	−56.55			44712.730	6.20
46341.801	12.56	47086.898	13.56	49270.043	−56.11	**HD 58385**		45284.020	2.86
46704.973	12.12	47196.715	14.27	50129.789	−57.78	45367.883	68.89	45367.902	5.40
46714.828	12.70	47789.938	11.81	50142.727	−56.73	45384.789	68.85	45410.855	4.07
46990.969	14.39	48232.832	13.97			45410.793	69.44	45452.777	3.36
47086.879	11.07	49262.035	13.14	**HD 52432**		45668.055	67.81	45668.078	4.43
47763.980	12.47	49695.797	10.40	44607.883	24.30	45712.812	71.04	45712.906	5.49
47872.758	12.39	50129.609	14.88	44712.695	25.47	46467.812	70.35	45752.902	4.30
49240.863	12.93	50142.688	15.42	44877.027	23.93	47087.035	70.88	45852.730	3.83
49261.938	12.35			45046.742	22.61	47260.770	68.97	46110.914	4.22
49647.801	12.73	**HD 286436**		45051.715	22.39	47872.980	70.99	46875.777	4.08
49695.715	12.98	45597.996	−33.98	45284.004	20.31	48951.035	66.01	47086.969	2.58
50129.664	12.23	45669.812	−34.22	45384.766	22.17	50123.812	68.57	47260.793	5.18
		46467.715	−34.75	45410.742	22.89	50142.824	68.50	47873.062	5.31
HD 16115		46714.863	−34.66	45452.719	24.34			48951.043	5.34
44876.914	15.29	47031.910	−35.50	45613.016	23.70	**HD 59643**		50115.875	6.05
44935.762	15.96	47086.906	−34.71	45668.047	21.28	45384.805	41.19	50128.828	4.48
45207.988	14.67	47789.926	−33.75	45669.938	21.55	45410.812	43.02		
45283.922	15.26	47872.805	−35.07	45712.801	22.10	45452.746	39.52	**HD 79319**	
45384.617	15.54	49262.012	−33.37	46467.777	21.78	45613.027	38.42	44304.832	−0.76
45597.949	14.55	49695.824	−34.51	46715.016	23.55	45670.074	39.22	44331.812	−1.22
45669.770	15.05	50112.707	−33.88	47086.930	22.22	45712.875	41.01	44607.953	−3.22
45989.852	14.73	50129.730	−34.90	47872.961	25.26	47086.949	38.75	44668.852	−2.98
46341.809	13.96	50142.703	−33.28	48951.000	23.83	47260.781	40.76	44683.863	−1.44
46704.980	15.45			50129.824	24.46	47873.039	44.75	44712.703	−0.19
47031.977	13.87	**BD+23 601**		50142.738	24.82	50123.848	49.30	45053.832	−2.70
47086.887	14.48	45598.012	−11.88					45284.035	−2.82
47789.918	14.96	45669.977	−10.99					45367.922	−3.48

Table 1—Continued

JD −2400000	RV km s^{-1}	JD −2400000	RV km s^{-1}	JD −2400000	RV km s^{-1}	JD −2400000	RV km s^{-1}	JD −2400000	RV km s^{-1}
HD 79319		**HD 122547**		**BD+23 2998**		**BD+17 3325**		**HD 197604**	
45410.848	−3.04	45803.926	−27.20	49560.816	−32.14	48019.953	−48.12	46657.863	15.73
45452.766	−3.05	46234.891	−28.03	50143.070	−31.13	48089.812	−48.13	46970.902	16.36
45668.086	−2.13	46657.711	−28.60			48467.859	−48.18	46990.875	16.36
45712.914	−2.58	46876.000	−28.55	**HD 156074**		49560.852	−48.49	47141.637	15.68
45752.906	−2.38	46970.777	−28.05	44305.035	−12.94	50129.062	−47.78	47763.883	17.07
45852.738	−2.49	47260.910	−29.00	44331.957	−12.44			47872.699	16.84
46110.926	−2.69	48467.746	−27.63	44382.852	−12.83	**HD 163838**		48162.734	15.46
46937.773	−4.39	49560.738	−27.70	44435.828	−12.19	45597.770	−41.65	48467.906	15.86
47087.020	−3.69	50128.953	−26.78	44482.738	−12.18	45667.645	−41.81	49175.828	16.43
47260.809	−1.47	50142.957	−26.63	44493.742	−12.62	45803.965	−41.42	49261.754	16.26
47873.098	−3.08			44668.984	−12.06	45915.918	−42.29	49560.922	15.87
48951.047	−3.67	**BD+30 2637**		44712.980	−13.43	46341.715	−43.34		
50126.836	−3.13	45597.691	−95.94	44781.824	−12.84	46657.801	−43.57	**BD+02 4338**	
50127.844	−3.18	45713.062	−96.71	44870.641	−12.45	46937.879	−42.72	45667.664	−52.48
50128.844	−2.44	45803.930	−96.74	44907.633	−12.97	46970.824	−42.26	45915.941	−53.38
		46242.820	−96.18	44935.590	−12.47	46990.848	−42.91	46341.734	−53.17
HD 85066		46341.660	−96.68	45171.742	−12.20	47057.770	−43.72	46657.871	−52.97
44331.828	−16.01	46657.746	−95.23	45207.688	−13.43	47260.996	−42.68	46970.906	−53.73
44683.883	−11.95	46876.031	−97.51	45284.645	−13.77	48019.965	−41.75	46990.879	−53.47
44712.742	−12.39	46970.770	−96.42	45452.891	−13.72	48089.824	−42.89	47141.645	−53.15
45284.031	−7.00	47031.773	−96.61	45597.758	−13.50	48387.973	−41.96	47763.934	−53.05
45367.914	−5.25	47057.688	−96.52	45803.945	−13.44	48467.887	−42.73	47872.648	−53.96
45410.859	−6.41	47142.074	−96.84	45915.789	−12.80	49175.855	−42.19	48162.742	−53.34
45452.789	−6.47	47260.973	−95.83	46111.027	−13.37	49560.875	−43.05	48467.914	−52.82
45668.094	−5.72	48019.891	−96.36	46242.879	−13.13	50129.070	−43.20	49175.840	−52.97
45712.926	−6.78	48089.773	−96.71	46341.707	−12.96			49261.766	−52.97
45752.898	−6.65	48387.887	−96.51	46657.777	−13.33	**HD 168227**		49560.930	−53.15
45852.746	−8.61	48467.754	−96.18	46937.828	−13.51	46242.863	−14.43		
46937.801	−18.63	49560.723	−96.51	46970.805	−12.36	46341.699	−14.78	**HD 218851**	
47031.785	−18.21	50128.969	−96.01	46990.824	−12.60	46657.816	−11.40	45597.828	−42.76
47087.012	−17.74	50143.016	−95.55	47141.660	−12.61	46970.859	−10.64	45667.820	−42.49
47142.031	−17.13			48019.941	−12.45	46990.867	−9.98	46341.746	−41.94
47260.801	−15.73	**BD+83 442**		48089.816	−13.03	47261.004	−11.36	46412.574	−42.62
47316.777	−14.73	45597.754	−16.10	48387.945	−12.69	48019.977	−11.79	46657.887	−41.97
48951.066	−12.50	45667.609	−15.63	48467.852	−12.58	48089.797	−10.53	46970.961	−42.73
50115.930	−16.36	45803.938	−16.02	49155.844	−12.70	48162.719	−9.75	46990.887	−42.72
50128.867	−16.08	46110.965	−15.94	49560.836	−12.64	48467.867	−12.26	47086.977	−43.30
50142.910	−15.75	46341.672	−15.55	50129.027	−12.78	49216.809	−11.11	47763.891	−44.21
		46657.758	−15.84	50143.078	−12.63	49560.891	−12.71	47872.730	−42.80
BD+02 2446		46876.043	−15.74					48162.801	−42.69
45712.938	10.23	46970.785	−15.77	**BD+02 3336**		**BD+28 3530**		48467.922	−42.43
45852.754	10.50	46990.816	−15.71	45597.727	−21.19	45597.797	−4.92	49175.844	−41.80
46937.816	9.67	47057.754	−16.07	45803.953	−34.46	45667.633	−5.19	49261.789	−41.58
46970.754	9.61	47087.027	−15.92	46242.840	−36.26	45915.902	−4.57	49560.973	−43.09
47141.973	10.63	47260.977	−16.08	46341.688	−22.87	46341.723	−5.23		
47260.812	10.62	48019.930	−15.65	46657.785	−38.69	46657.836	−5.43	**HD 223392**	
48019.828	11.42	48089.781	−15.81	46937.836	−22.85	46970.867	−4.42	44485.828	−19.90
50123.953	11.33	48387.957	−13.32	46970.809	−26.60	46990.871	−4.45	44870.805	−19.68
50128.902	10.47	49155.887	−15.45	46990.836	−29.86	47057.805	−5.22	44907.668	−19.69
		50128.996	−16.37	47260.984	−19.45	47763.879	−4.89	44935.727	−20.12
BD+04 2735		50143.039	−15.76	48019.949	−35.99	47872.672	−7.73	45207.902	−20.31
45713.039	−15.07			48089.793	−26.74	48089.859	−4.74	45597.836	−21.35
45803.914	−14.92	**BD+23 2998**		48467.828	−35.42	48162.730	−4.87	45667.684	−20.51
45849.824	−13.94	45597.719	−32.02	49155.930	−20.61	48467.895	−4.28	45915.949	−20.21
46242.816	−15.72	45803.941	−31.87	49560.844	−17.19	49175.809	−4.36	46341.746	−20.75
46937.824	−15.68	45915.797	−30.99	50143.090	−33.27	49261.715	−4.71	46657.930	−20.87
46970.742	−14.88	46242.828	−32.01			49560.906	−5.09	46990.895	−21.17
47142.039	−14.42	46341.680	−31.85	**BD+17 3325**				47031.832	−21.08
47260.906	−14.99	46657.770	−31.69	45597.746	−48.28	**HD 197604**		47141.656	−20.49
48019.812	−14.56	46876.055	−31.98	45803.957	−48.56	44482.797	16.44	47763.938	−20.58
48089.770	−14.70	46970.789	−31.49	45915.887	−47.10	44781.855	17.00	47872.715	−20.99
48387.855	−14.79	47057.727	−31.46	46242.852	−48.04	44870.719	16.96	48162.809	−21.33
50128.961	−15.17	47142.086	−32.33	46341.691	−47.83	44907.641	16.14	48467.926	−20.36
50142.941	−15.06	47316.848	−31.72	46657.793	−48.28	44935.605	15.64	49261.801	−20.36
		48019.938	−31.59	46937.844	−48.18	45207.719	16.97	49560.980	−20.91
HD 122547		48089.785	−31.83	46970.816	−48.65	45597.809	16.92		
44668.953	−26.52	48387.930	−31.56	46990.840	−47.84	45667.812	16.35		
45368.066	−27.45	48467.809	−31.48	47057.738	−47.82	45915.934	15.77		

Table 2. Carbon Star Sample

Star	Sp. Class	Ref.
HD 1994	R5, J4.5	1
BD +29°95	CH	2
BD +21°64	R2	3
HD 16115	R3, CH3	3,1
HD 19557	R5, J4	1
HD 19881	N5+	1
HD 286436	R2	3
BD +23°601	R2	3
HD 34467	Nb	3
HD 37212	N4	1
BD +33°1194	R2	3
HD 52432	R5, J3.5	3,1
HD 57884	R8	3
HD 58337	R3	3
HD 58364	R3	3
HD 58385	N	3
HD 59643	R9	3
HD 63353	R8	3
HD 76846	R2+	1
HD 77234	R5	3
HD 79319	R4	3
HD 85066	R3, CH	3,4
BD +2°2446	R2	3
BD +4°2735	R0	3
HD 122547	R2	3
BD +30°2637	R0	3
BD +83°442	R0	3
BD +23°2998	R2.5	1
HD 156074	R2	1
BD +2°3336	CH, N4	2,1
BD +17°3325	R0	3
HD 163838	R4	3
HD 168227	R5	3
BD +28°3530	R0	3
HD 197604	CH	2
BD +2°4338	R2	3
HD 218851	R2	3
HD 223392	R3	3

References. — (1) Keenan 1993; Barnbaum et al. 1996 (2) Yamashita 1975a (3) Shane 1928; Sanford 1944; Vandervort 1958; Yamashita 1972, 1975b; Stephenson 1973 (4) Hartwick and Cowley 1985

Table 3. Orbital Elements for CH Stars

Element	HD 85066	BD +02°3336
P (days)	2901.7±19.1	445.94±0.61
γ (km s^{-1})	−13.09±0.25	−27.46±0.22
K (km s^{-1})	7.40±0.40	10.54±0.29
e	0.21±0.04	0.03±0.03
ω (^{0})	93.9±8.7	162.1±41.0
T (JD−2400000^d)	46094.4±61.8	47064.2±51.0
$a \sin i$ (Gm)	288.5±15.8	64.6±1.8
f(m) ($M_\odot$)	0.1129±0.0186	0.0541±0.0045

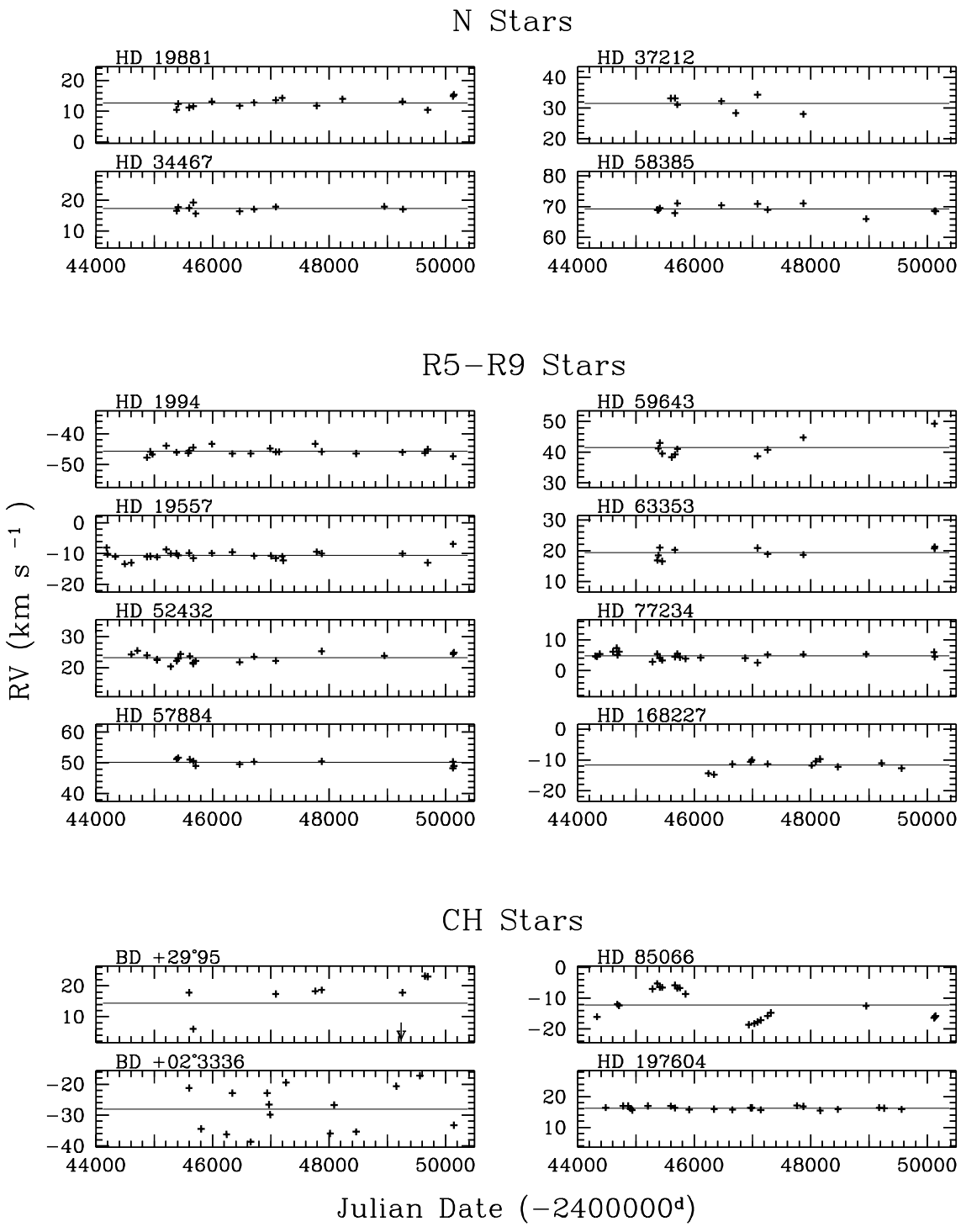

Fig. 1.— Radial Velocities versus Julian Dates for stars in the sample that have modern classifications of N, R5-R9, or CH-like.

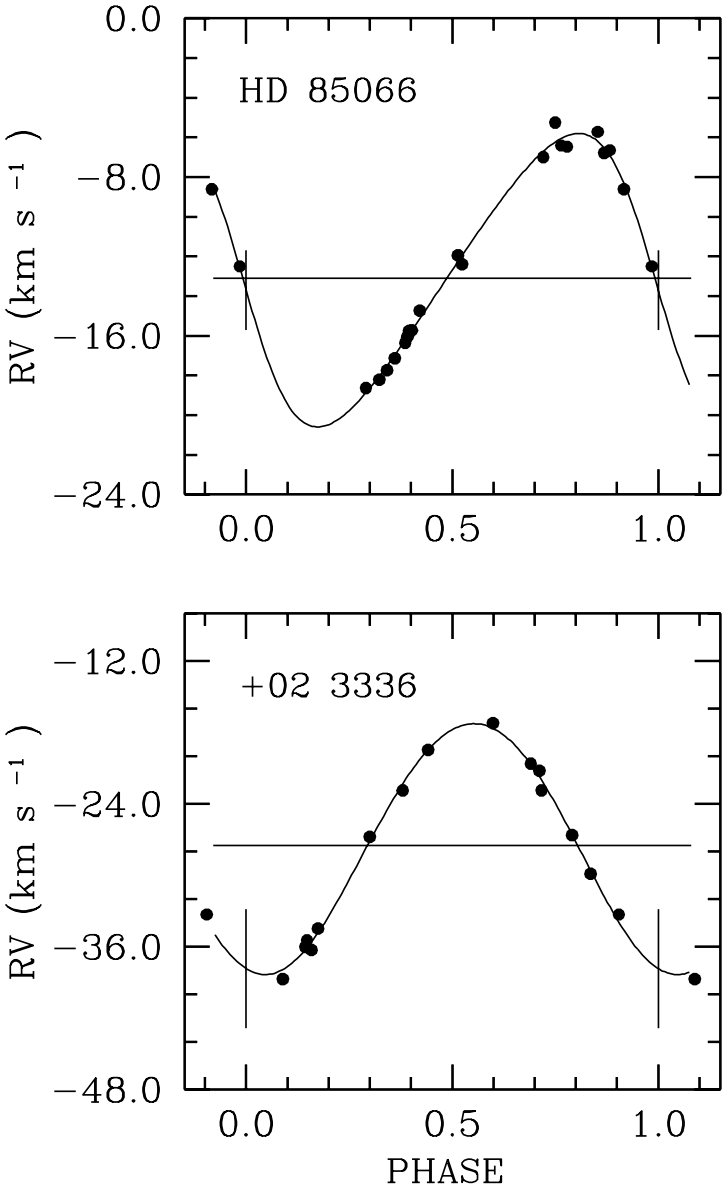

Fig. 2.— Radial Velocities versus Phase for the computed orbits (solid curves) from the elements listed in Table 3. The observed velocities from which these orbits were calculated are plotted as dots.

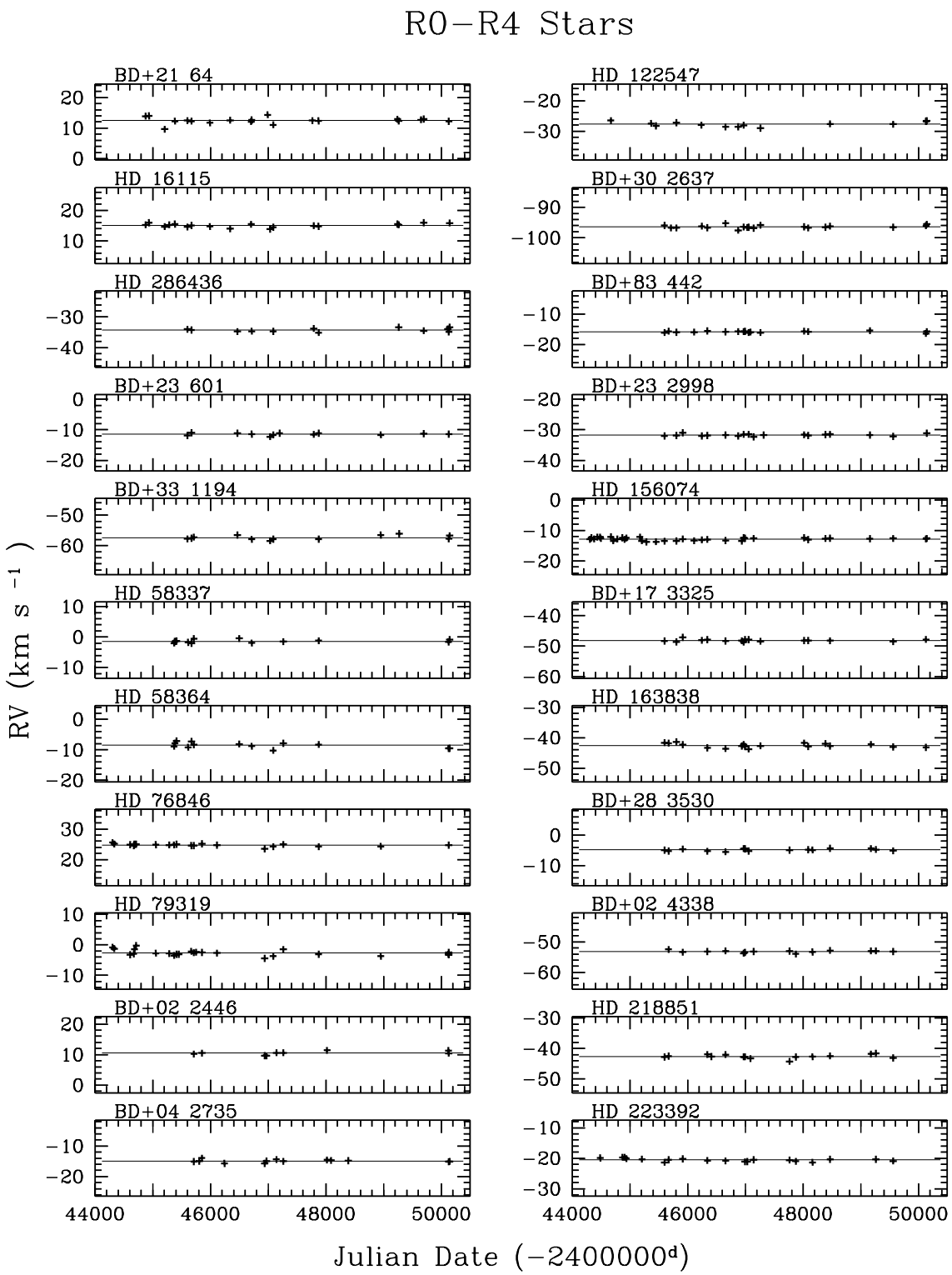

Fig. 3.— Radial Velocities versus Julian Dates for the remaining R0−R4 stars in the sample.

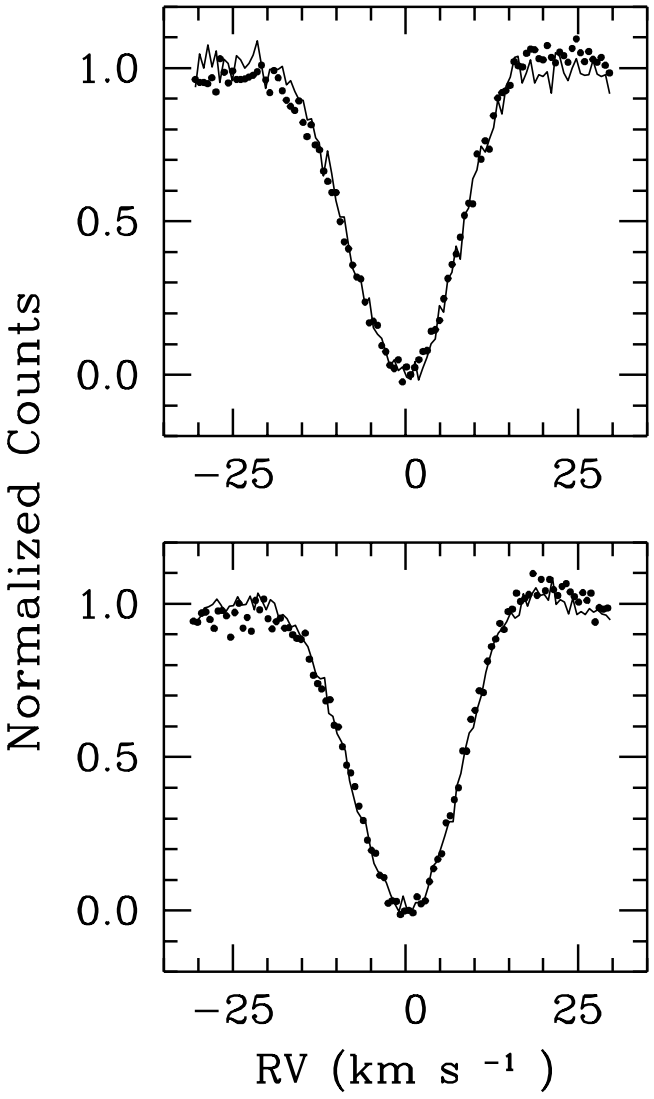

Fig. 4.— Comparison of cross-correlation profiles from the radial-velocity spectrometer for two pairs of R stars (dots) versus normal K giants (solid curves). The profiles have been normalized to a continuum level of 1.0, a minimum of 0.0, and centered on radial-velocity of 0.0. The profiles are from the R stars are HD 156074 (left) and BD +17°3325 (right), and the K giants are HD 134493 (left) and HD 154391 (right).